A Variational Formulation for Nonconforming Sliding Interfaces in Finite Element Analysis of Electric Machines

Enno Lange, François Henrotte, and Kay Hameyer

Institute of Electrical Machines-RWTH Aachen University, D-52056 Aachen, Germany

This paper proposes the application of the Lagrange multiplier method to implement the relative motion of stator and rotor in the finite element (FE) simulations of electric machines. The nonconformity at the interface between stator and rotor regions imposes no restriction on time or space discretization. This freedom is highly valuable for domain decomposition. Through the choice of particular dual shape functions for the Lagrange multiplier, the symmetry, sparsity and positive definiteness of the linear system can be preserved. The method is applied to the 2-D simulation of a permanent magnet excited synchronous machine, and the results are compared with a conforming moving band approach with re-meshing of the air gap.

***Index Terms*—Bi-orthogonal shape functions, electric machines, finite element methods, sliding interfaces.**

I. Introduction

SEVERAL approaches to simulate the movement within a finite element analysis (FEA) of electrical machines have been developed. Static and transient analysis of the machines require a flexible variation of the rotor position. An obvious and early adopted approach is the moving band (MB) technique [4] whose principle is to re-generate at each time step a single layer of conforming finite elements in a thin annulus-shaped region of the air gap. However, in practice, air gap re-meshing can be done automatically for 2-D rotating machines only. For linear motion in 2-D and motion in 3-D models, air gap re-meshing would imply invoking a full-fledged automatic mesh generator at each time step, which is impractical. The mortar element method (MEM) was proposed in [8] and applied to a 2-D machine problem in [1]. The Lagrange multiplier (LM) method has been extensively investigated in [2]. Both MEM and LM can be extended to 3-D problems, but the MEM requires an additional integration mesh [9], and for the LM the conditioning worsens significantly [6].

The nonconforming approach presented in this paper is based on the LM method, but instead of using the standard nodal basis functions for the discrete Lagrange multiplier, the basis functions fulfill the bi-orthogonality relation proposed in [11]. This makes it possible to eliminate the Lagrange multiplier by a discrete projection operator, and the resulting linear system is symmetric positive definite.

II. Variational Formulation

Let Ω^m and Ω^s be the master and the slave domain respectively, e.g., the stator and rotor of an electric machine. The choice of the domains is arbitrary but fixed. Let $\Gamma^m \subset \partial\Omega^m$ and $\Gamma^s \subset \partial\Omega^s$ be the sliding interface between the master and the slave domain and $p : \Gamma^s \to \Gamma^m$ be a smooth mapping that may account for a relative motion between the stator and the rotor, i.e., the master and the slave domain.

Assuming for simplicity reasons homogeneous Dirichlet boundary conditions on $\partial\Omega^m \setminus \Gamma^m \cup \partial\Omega^s \setminus \Gamma^s$ (Neumann boundary conditions would be treated in the classical way), the energy balance of the system reads [7]

$$\delta \sum_{k=m,s} \left(\Psi^k(\mathrm{curl}\mathbf{A}^k) - \int_{\Omega^k} \mathbf{J}^k \mathbf{A}^k \mathrm{d}\Omega^k \right) + \delta \int_{\Gamma^s} \boldsymbol{\lambda} \cdot (\mathbf{A}^s - \mathbf{A}^m \circ p) \mathrm{d}\Gamma^s = 0 \quad (1)$$

where Ψ^k represents the magnetic energy of the domain $k = m, s$, which is a function of the flux density $\mathbf{B}^k = \mathrm{curl}\mathbf{A}^k$ with $\mathbf{A}^k$ the magnetic vector potential. The second term is the magnetic work delivered by the current density $\mathbf{J^k}$. The third term, with the Lagrange multiplier $\boldsymbol{\lambda}$, is a penalty term ensuring the continuity of the magnetic vector potential across the sliding interface $\Gamma^m = p\Gamma^s$.

Applying the variation operator, one obtains the weak formulation, i.e., the equation

$$\sum_{k=m,s} \int_{\Omega^k} (\mathbf{H}^k \mathrm{curl}\delta\mathbf{A}^k - \mathbf{J}^k \delta\mathbf{A}^k) \mathrm{d}\Omega^k + \int_{\Gamma^s} \times \{\delta\boldsymbol{\lambda}(\mathbf{A}^s - \mathbf{A}^m \circ p) + \boldsymbol{\lambda}(\delta\mathbf{A}^s - \delta\mathbf{A}^m \circ p)\} \mathrm{d}\Gamma^s = 0 \quad (2)$$

which must be verified for arbitrary variations $\delta\mathbf{A}^k$ and $\delta\boldsymbol{\lambda}$ fulfilling the boundary conditions.

A. Euler–Lagrange Equations

Before discretizing (2) as described in Section II-B, a closer look on the continuity of the fields and the physical meaning of the Lagrange multiplier $\boldsymbol{\lambda}$ provides a deeper insight into the formulation. For the sake of clarity, the sliding interface Γ is assumed not to intersect with a Dirichlet or any other boundary condition, e.g., (anti-)symmetries, and Γ is assumed being a simply connected region. Applying Stoke's theorem

$$\begin{aligned} &\sum_{k=m,s} \int_{\Omega^k} (\mathrm{curl}\mathbf{H}^k - \mathbf{J}^k) \delta\mathbf{A}^k \mathrm{d}\Omega^k \\ &- \sum_{k=m,s} \int_{\Gamma^k} \mathbf{H}^k \times \delta\mathbf{A}^k \cdot \mathbf{n}^k \mathrm{d}\Gamma^k \\ &+ \int_{\Gamma^s} \boldsymbol{\lambda} \delta\mathbf{A}^s \mathrm{d}\Gamma^s - \int_{\Gamma^m} \boldsymbol{\lambda} \circ p^{-1} \delta\mathbf{A}^m \mathrm{d}\Gamma^m \\ &+ \int_{\Gamma^s} \delta\boldsymbol{\lambda}(\mathbf{A}^s - \mathbf{A}^m \circ p) \mathrm{d}\Gamma^s = 0 \end{aligned} \quad (3)$$

Manuscript received December 23, 2009; accepted January 29, 2010. Current version published July 21, 2010. Corresponding author: E. Lange (e-mail: enno.lange@iem.rwth-aachen.de).

Color versions of one or more of the figures in this paper are available online at http://ieeexplore.ieee.org.

Digital Object Identifier 10.1109/TMAG.2010.2043075

leads to

$$\sum_{k=m,s}\int_{\Omega^k}(\mathrm{curl}\mathbf{H}^k-\mathbf{J}^k)\delta\mathbf{A}^k\mathrm{d}\Omega^k + \int_{\Gamma^s}(\boldsymbol{\lambda}-\mathbf{n}^s\times\mathbf{H}^s)\delta\mathbf{A}^s\mathrm{d}\Gamma^s - \int_{\Gamma^m}(\boldsymbol{\lambda}\circ p^{-1}+\mathbf{n}^m\times\mathbf{H}^m)\delta\mathbf{A}^m\mathrm{d}\Gamma^s + \int_{\Gamma^s}\delta\boldsymbol{\lambda}(\mathbf{A}^s-\mathbf{A}^m\circ p)\mathrm{d}\Gamma^s=0. \quad (4)$$

The variables $\mathbf{A}^m$, $\mathbf{A}^s$ and $\boldsymbol{\lambda}$, being linearly independent, their variations are arbitrary. The Euler–Lagrange equations of the variational formulation are

$$\mathrm{curl}\mathbf{H}^k=\mathbf{J}^k \quad \text{in } \Omega^k \text{ with } k=m,s \quad (5)$$
$$\mathbf{n}^s\times\mathbf{H}^s=\boldsymbol{\lambda} \quad \text{on } \Gamma^s \quad (6)$$
$$\mathbf{n}^m\times\mathbf{H}^m=-\boldsymbol{\lambda}\circ p^{-1} \quad \text{on } \Gamma^m=p\Gamma^s \quad (7)$$
$$\mathbf{A}^s=\mathbf{A}^m\circ p \quad \text{on } \Gamma^s. \quad (8)$$

Ampere's law is given by (5). The continuity of the fields $\mathbf{H}^k$ and $\mathbf{A}^k$ is ensured by (6)–(8), whereas the physical interpretation of the Lagrange multiplier $\boldsymbol{\lambda}$ is given by (6) and (7), where the tangential component $\mathbf{H}_t^k$ of the magnetic field on the sliding interface $\Gamma^m=p\Gamma^s$ equals the Lagrange multiplier $\boldsymbol{\lambda}$ with respect to the in- and outward direction of the normal vector $\mathbf{n}^k$.

B. Discretization

Following the usual discretization approach, the magnetic vector potentials for the master and slave domain, and the Lagrange multiplier are approximated by

$$\mathbf{A}^k=\sum_l A_l^k\boldsymbol{\alpha}_l^k, \qquad \delta\mathbf{A}^k=\{\boldsymbol{\alpha}_l^k\} \quad (9)$$
$$\boldsymbol{\lambda}=\sum_j\lambda_j\boldsymbol{\mu}_j, \qquad \delta\boldsymbol{\lambda}=\{\boldsymbol{\mu}_j\}. \quad (10)$$

The field $\mathbf{A}$ is discretized with nodal shape functions in 2-D and edge shape functions in 3-D. For $\boldsymbol{\mu}_j$ is defined on Γ^s only, the superscript ^{s} is omitted. In both cases, the functional spaces of the variations $\delta\mathbf{A}^k$ and $\delta\boldsymbol{\lambda}$ are spanned by the shape functions of all nodes, or edges, not subject to a Dirichlet boundary condition. The choice of the shape functions of the Lagrange multiplier $\boldsymbol{\mu}_j$ is discussed in Section III.

In order to establish the FE equations in matrix form, the vectors of the unknown fields $\mathbf{A}^k$ are divided into two blocks each. The first block $\mathbf{A}_\Gamma^k$ contains the unknowns lying on the sliding interface Γ^k. The second block $\mathbf{A}_i^k$ contains the unknowns lying in the interior of the domain Ω^k. The vectors of unknowns then become

$$\mathbf{A}^m=\begin{pmatrix}\mathbf{A}_i^m\\ \mathbf{A}_\Gamma^m\end{pmatrix}, \quad \mathbf{A}^s=\begin{pmatrix}\mathbf{A}_\Gamma^s\\ \mathbf{A}_i^s\end{pmatrix}. \quad (11)$$

Equation (2) yields then the saddle-point problem

$$\begin{pmatrix}\mathbf{S}_{i,i}^m & \mathbf{S}_{i,\Gamma}^m & 0 & 0 & 0\\ \mathbf{S}_{\Gamma,i}^m & \mathbf{S}_{\Gamma,\Gamma}^m & 0 & 0 & -\mathbf{M}^T\\ 0 & 0 & \mathbf{S}_{\Gamma,\Gamma}^s & \mathbf{S}_{\Gamma,i}^s & \mathbf{D}^T\\ 0 & 0 & \mathbf{S}_{i,\Gamma}^s & \mathbf{S}_{i,i}^s & 0\\ 0 & -\mathbf{M} & \mathbf{D} & 0 & 0\end{pmatrix}\begin{pmatrix}\mathbf{A}_i^m\\ \mathbf{A}_\Gamma^m\\ \mathbf{A}_\Gamma^s\\ \mathbf{A}_i^s\\ \boldsymbol{\lambda}\end{pmatrix}=\begin{pmatrix}\mathbf{b}^m\\ 0\\ 0\\ \mathbf{b}^s\\ 0\end{pmatrix} \quad (12)$$

with the FE matrices

$$\mathbf{S}_{ln}=\sum_{k=m,s}\int_{\Omega^k}\nu\mathrm{curl}\boldsymbol{\alpha}_l^k\mathrm{curl}\boldsymbol{\alpha}_n^k\mathrm{d}\Omega^k \quad (13)$$
$$\mathbf{b}_l=\sum_{k=m,s}\int_{\Omega^k}\mathbf{J}\boldsymbol{\alpha}_l^k\mathrm{d}\Omega^k \quad (14)$$
$$\mathbf{D}_{jl}=\int_{\Gamma^s}\boldsymbol{\mu}_j\boldsymbol{\alpha}_l^s\mathrm{d}\Gamma^s \quad (15)$$
$$\mathbf{M}_{jl}=\int_{\Gamma^s}\boldsymbol{\mu}_j\boldsymbol{\alpha}_l^m\circ p\mathrm{d}\Gamma^s \quad (16)$$

i.e., the stiffness matrix $\mathbf{S}$ with the magnetic reluctivity ν, the right hand-side $\mathbf{b}$, and the coupling matrices $\mathbf{D}$ and $\mathbf{M}$ arising from the discrete Lagrange multiplier.

In order to obtain a symmetric positive definite system, the degrees of freedom $\mathbf{A}_\Gamma^s$ associated to the slave side Γ^s of the sliding interface are eliminated thanks to the last block-line of the saddle-point system (12) and expressed by a linear combination of $\mathbf{A}_\Gamma^m$

$$\mathbf{D}\mathbf{A}_\Gamma^s-\mathbf{M}\mathbf{A}_\Gamma^m=0 \quad (17)$$
$$\mathbf{A}_\Gamma^s=\mathbf{D}^{-1}\mathbf{M}\mathbf{A}_\Gamma^m. \quad (18)$$

Now

$$\mathbf{Q}=:\mathbf{D}^{-1}\mathbf{M}\equiv\left(\mathbf{M}^T\mathbf{D}^{-T}\right)^T \quad (19)$$

can be identified as a discrete projection operator. From the third line of (12) the Lagrange multiplier can be extracted

$$\boldsymbol{\lambda}=-\mathbf{D}^{-T}\mathbf{S}_{\Gamma,\Gamma}^s\mathbf{D}^{-1}\mathbf{M}\mathbf{A}_\Gamma^m-\mathbf{D}^{-T}\mathbf{S}_{\Gamma,i}^s\mathbf{A}_i^s. \quad (20)$$

Inserting (18) and (20) in (12) one yields the reduced equation system with the projection operator (19)

$$\begin{pmatrix}\mathbf{S}_{i,i}^m & \mathbf{S}_{i,\Gamma}^m & 0\\ \mathbf{S}_{\Gamma,i}^m & \mathbf{S}_{\Gamma,\Gamma}^m+\mathbf{Q}^T\mathbf{S}_{\Gamma,\Gamma}^s\mathbf{Q} & \mathbf{Q}^T\mathbf{S}_{\Gamma,i}^s\\ 0 & \mathbf{S}_{i,\Gamma}^s\mathbf{Q} & \mathbf{S}_{i,i}^s\end{pmatrix}\begin{pmatrix}\mathbf{A}_i^m\\ \mathbf{A}_\Gamma^m\\ \mathbf{A}_i^s\end{pmatrix}=\begin{pmatrix}\mathbf{b}^m\\ 0\\ \mathbf{b}^s\end{pmatrix}. \quad (21)$$

The equation system (21) is symmetric positive definite and may be treated by standard Krylov subspace methods. However, to obtain (21) one is required to calculate $\mathbf{D}^{-1}$, which can be seen in (19). As (15) shows, the structure of $\mathbf{D}$ depends on the choice of the shape functions $\boldsymbol{\mu}$ of the Lagrange multiplier $\boldsymbol{\lambda}$, and thus, either $\mathbf{D}^{-1}$ must be calculated explicitly in a step prior to solving (21) or an appropriate choice of the function space of $\boldsymbol{\mu}$ in (10) allows for an implicit inversion during the assembly of (19). Note that up to this point no restrictions regarding the dimension of the domains have been made.

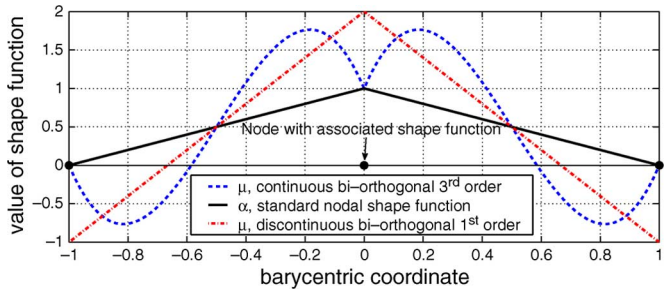

Fig. 1. Standard nodal shape function, discontinuous and continuous bi-orthogonal dual shape function for a 1-D interface in Γ.

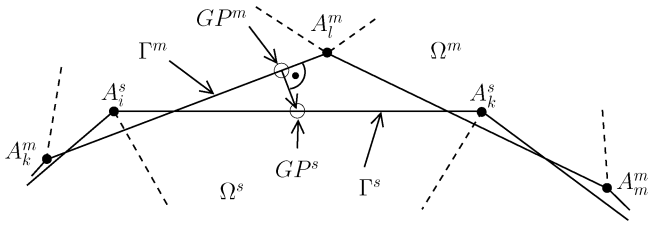

Fig. 2. Simplified intersection of master Ω^m and slave Ω^s domain and integration points GP^s on Γ^s and $GP^m \neq p_\theta(GP^s)$ on Γ^m.

III. Bi-Orthogonal Shape Functions

From the practical point of view, the inversion of $\mathbf{D}$ must be carried out each time the mapping p changes. Thus, unless the number of degrees of freedom associated with Γ^s is considerably smaller than the total number of DoFs, or unless $\mathbf{D}$ is a diagonal matrix, this inversion is rather expensive in terms of computation time. Since the number of degrees of freedom on Γ^s is problem-dependent, one could advantageously seek a way to diagonalize $\mathbf{D}$. The diagonalization can be achieved be choosing the basis functions $\boldsymbol{\mu}$ for $\boldsymbol{\lambda}$ in a dual function space, as proposed in [3], [11] and successfully applied in [5], so that the bi-orthogonality relation

$$\mathbf{D} = \int_{\Gamma^s} \mu_j \alpha_l^s \mathrm{d}\Gamma^s = \delta_{jl} \int_{\Gamma^s} \alpha_l^s \mathrm{d}\Gamma^s, \quad \text{with } \delta_{jl} = \begin{cases} 1, & \text{if } j = l \\ 0, & \text{if } j \neq l \end{cases} \tag{22}$$

is fulfilled. Thanks to (22), the inversion of $\mathbf{D}$ is trivial and the discrete projection operator $\mathbf{Q}$ can be applied implicitly during the standard element-wise assembly of (21).

For a 1-D interface Γ, two possible choices of dual basis functions are depicted in Fig. 1. The discontinuous shape function (first polynomial order) might result in a loss of accuracy if the numerical integration is not adapted to the discontinuities. Since the discretizations of the master and the slave meshes are independent, the discontinuities of the Lagrange multiplier shape functions are not taken into account by numerical integration on the master side. Therefore, [12] proposes continuous Lagrange multiplier basis functions as shown in Fig. 1. The continuous shape functions are of third polynomial order. Their numerical integration, compared to the discontinuous shape functions of first order, require a slightly higher computational effort. Anyhow, numerical experiments have not revealed any disadvantages in using the discontinuous basis functions.

IV. Implementation Aspects

The described approach has been implemented within the FEM-package *i*MOOSE [10]. In rotational motion problems, discretization inevitably polygonizes the interfaces Γ^m and Γ^s, Fig. 2.

The simple rotation mapping

$$p_\theta : (x^s, y^s) \mapsto (\sin(\theta(t))\, x^s, \cos(\theta(t))\, y^s) \tag{23}$$

is, therefore, in general, not a mapping $\Gamma^s \mapsto \Gamma^m$ as it should be, i.e., the image $p_\theta(GP^s)$ of the integration Gauss point GP^s is not found on Γ^m. A straightforward solution is to define GP^m as the orthogonal projection of $p_\theta(GP^s)$ on Γ^m. This minimizes the distance between GP^m and $p_\theta(GP^s)$. The required mapping $p : \Gamma^s \mapsto \Gamma^m$ is thus the composition of this projection with p_θ. The shape function α^m can then be evaluated at $GP^m = p(GP^s) \in \Gamma^m$. Since the integrand in (16) is no longer C^0-continuity, it is advisable to use more integration points than for C^0-continuity.

V. Application

As an application example, the 2-D quasi-static field problem of a permanent magnet excited synchronous machine has been examined. The sliding interface is located on an annulus-shaped cylinder around the rotation axis in the air gap. Equal mesh sizes on the sliding interface Γ between stator and rotor domain as well as different mesh sizes have been analyzed, as shown in Fig. 3, where the size of the elements on Γ^s is about one fourth of the size of the elements on Γ^m. One can clearly see that both the normal and the tangential component of the induction field are continuous across Γ, as expected in the case of an identical reluctivity ν_0 on both sides of the interface. Indeed, the vector potential is continuous, i.e., the field lines match (continuity of B_n), and the tangents of the field lines also match at the interface (continuity of H_t).

A closer look at the tangential component of the magnetic field $|\mathbf{H}_t|$ is depicted in Fig. 4. Herein, the absolute value of the tangential component $|\mathbf{H_t}|$ on the moving band interface Γ of a conformal discretization is compared to the tangential component $|\mathbf{H}_t^m|$ and $|\mathbf{H}_t^s|$ on Γ^m and Γ^s. A good agreement between the conformal and the presented nonconforming approach is observed.

VI. Conclusion

In this work, a Lagrange multiplier is applied to ensure the continuity of the magnetic vector potential and the tangential component of the magnetic field on a nonconforming interface between two separated domains. The degrees of freedom on the slave side of the interface are replaced by a motion-dependent linear combination of degrees of freedom of the master side. Then, by choice of the function space of the discrete Lagrange multiplier dual to the discrete function space of the field fulfilling the bi-orthogonality relation, the Lagrange multiplier is

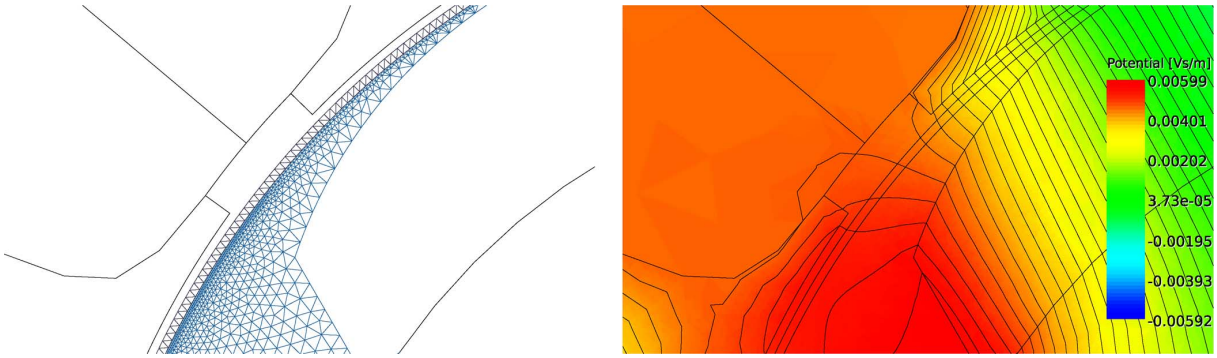

Fig. 3. Simulation results of a PMSM: Coarse mesh size on Γ^m and a finer mesh size on Γ^s and the calculated magnetic vector potential with flux lines.

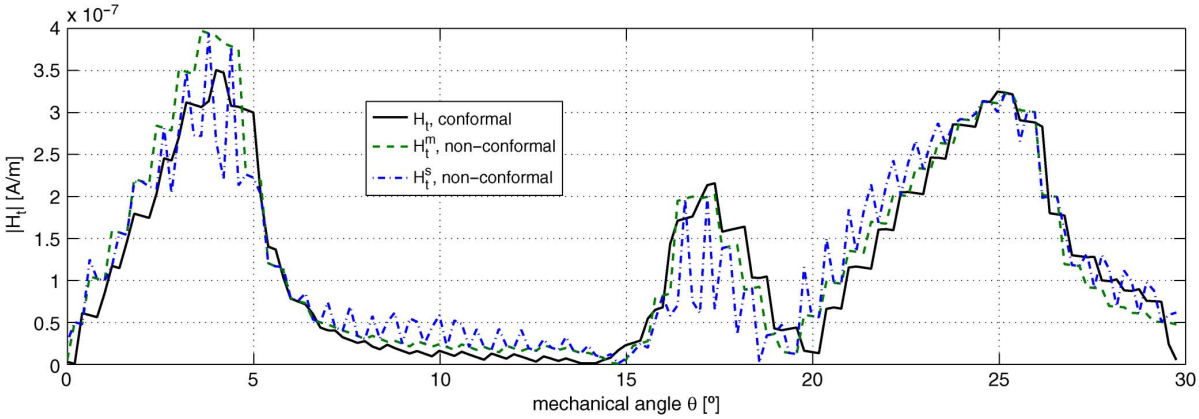

Fig. 4. Tangential component $|\mathbf{H}_t|$ of the magnetic field of a conforming and the presented nonconforming approach versus the circumferential angle θ.

eliminated, and the resulting equation system becomes symmetric positive definite. The presented approach has been successfully applied to a PMSM and the results are compared to a conformal discretization approach.

It should be noted that the mapping function may account for translational as well as rotational motions easing the burden of implementing different problem solvers for each type of motion. Furthermore, this work is a promising step towards a consistent 3-D formulation allowing for an easy to use implementation, avoiding, e.g., a time consuming re-meshing processes or the tedious handling of a lock-step method. The research now focuses on defining the dual function space of discrete Lagrange multiplier for 3-D tetrahedral edge elements.

REFERENCES

[1] O. Antunes, J. Bastos, N. Sadowski, A. Razek, L. Santandrea, F. Bouillault, and F. Rapetti, "Using hierarchic interpolation with mortar element method for electrical machines analysis," *IEEE Trans. Magn.*, vol. 41, no. 5, pp. 1472–1475, May 2005.

[2] O. Antunes, J. Bastos, N. Sadowski, A. Razek, L. Santandrea, F. Bouillault, and F. Rapetti, "Torque calculation with conforming and nonconforming movement interface," *IEEE Trans. Mag.*, vol. 42, no. 4, pp. 983–986, Apr. 2006.

[3] A. Buffa, Y. Maday, and F. Rapetti, "A sliding mesh-mortar method for a two dimensional eddy currents model of electric engines," *M2AN*, vol. 35, no. 2, pp. 191–228, Mar. 2001.

[4] B. Davat, Z. Ren, and M. Lajoie-Mazenc, "The movement in field modeling," *IEEE Trans. Magn.*, vol. MAG-21, no. 6, pp. 2296–2298, Nov. 1985.

[5] B. Flemisch and B. Wohlmuth, "Nonconforming discretization techniques for coupled problems," in *Multifield Problems in Solid and Fluid Mechanics*, R. Helmig, A. Mielke, and B. Wohlmuth, Eds. New York: Springer, 2006, vol. 28, Lecture notes in applied and computational mechanics, pp. 531–560.

[6] C. Golovanov, J.-L. Coulomb, Y. Marechal, and G. Meunier, "3-D mesh connection techniques applied to movement simulation," *IEEE Trans. Magn.*, vol. 34, no. 5, pp. 3359–3362, Sep. 1998.

[7] F. Henrotte and K. Hameyer, "The structure of electromagnetic energy flows in continuous media," *IEEE Trans. Magn.*, vol. 43, no. 4, pp. 903–906, Apr. 2006.

[8] F. Rapetti, E. Bouillault, L. Santandrea, A. Buffa, Y. Maday, and A. Razek, "Calculation of eddy currents with edge elements on non-matching grids in moving structures," *IEEE Trans. Magn.*, vol. 36, no. 4, pp. 1351–1355, Jul. 2000.

[9] F. Rapetti, Y. Maday, F. Bouillault, and A. Razek, "Eddy-current calculations in three-dimensional moving structures," *IEEE Trans. Magn.*, vol. 38, no. 2, pp. 613–616, Mar. 2002.

[10] D. van Riesen, C. Monzel, C. Kaehler, C. Schlensok, and G. Henneberger, "imoose-an open-source environment for finite-element calculations," *IEEE Trans. Magn.*, vol. 40, no. 2, pp. 1390–1393, Mar. 2004.

[11] B. I. Wohlmuth, "A mortar finite element method using dual spaces for the lagrange multiplier," *SIAM J. Numer. Anal.*, vol. 38, no. 3, pp. 989–1012, 2001.

[12] B. I. Wohlmuth, "A comparison of dual lagrange multiplier spaces for mortar finite element discretizations," *M2AN*, vol. 36, no. 6, pp. 995–1012, Nov. 2002.